J. Fluid Mech. (1966), *vol.* 26, *part* 1, *pp.* 49–68
Printed in Great Britain

Large-amplitude Bénard convection

By GEORGE VERONIS
Massachusetts Institute of Technology, Cambridge, Massachusetts

(Received 30 November 1965)

Calculations are presented for two-dimensional Bénard convection between free bounding surfaces for ranges of Rayleigh and Prandtl numbers. The variables are expanded in a series consisting of the eigenfunctions of the stability problem and the system is truncated to take into account only a limited number of terms. The amplitudes of the eigenfunctions are evaluated by numerical integration of the resulting non-linear equations. In all cases considered, the system achieves a steady state with the motion consisting of a single large cell. Results for Nusselt number *vs.* Rayleigh number are given for a range of Prandtl number varying between 0·01 and 100 and show that heat flux increases slightly with decreasing Prandtl number. The calculations agree with those of Kuo where the ranges of Rayleigh number overlap. A simple heuristic argument based on the assumption that turbulent boundary layers exist is also given and the conclusions of the latter indicate that heat flux should decrease with decreasing Prandtl number. Thus the behaviour is qualitatively different from that of the calculations. The reason appears to be associated with the fact that the single large cell in the computed cases enables the fluid to accelerate through repeated cycles until it achieves a steady state with the amplitude of the motion much larger than could be acquired by a single turbulent blob free-falling in the gravitational field.

1. Introduction

Two recent investigations have shown that, when a layer of fluid is heated uniformly from below and cooled from above, the resulting convection takes place as a pattern of two-dimensional rolls. Schlüter, Lortz & Büsse (1965) have treated the theoretical problem by taking as a basic state a fluid with a steady pattern of cellular motions and then perturbing the given pattern with an arbitrary disturbance. They showed that the only pattern which is stable to the perturbations is a system of convecting rolls.

In a recent seminar at Harvard University L. Koschmieder exhibited cellular patterns which were established under very carefully controlled conditions. When the fluid had a free upper surface, the resulting motion consisted of a remarkably uniform pattern of hexagons. When both boundaries were rigid, two-dimensional rolls were established. The influence of the shape of the lateral boundaries was reflected in the orientation of the rolls. When the boundaries were circular, the pattern consisted of concentric circular rolls (cylindrical symmetry). When the boundaries formed a square, the pattern tended to be straight rolls, although in this case each set of two parallel boundaries tended to establish two-dimensional rolls so that only in the region away from the boundaries did one of the sets of rolls

dominate. The principal point, however, is that convection did tend to establish itself as a two-dimensional pattern.

This paper contains a study of two-dimensional Bénard convection with the upper and lower boundaries free (slip). Although the latter boundary conditions are unrealizable in the laboratory, they may be more appropriate for large-scale geophysical and astrophysical phenomena where convective layers are most often bounded by a free surface or by a region of stable fluid. The rigid-boundary case is also being investigated and will be reported later.

In the following three sections the procedure for solving the two-dimensional problem is described. Briefly, the method involves an analysis of the different fields by means of a truncated Fourier set (for this problem this is equivalent to a truncated set of eigenfunctions). Once the external parameters are given it is possible, in principle, to derive a solution which is valid to any preassigned order of accuracy. Practically, there is a limitation to the values of the parameters which can be treated. These limits are discussed in connexion with specific problems.

In § 5 we discuss the solutions which have been obtained for ordinary Bénard convection by means of the method proposed in §§ 2–4. We deduce information about the situation where the rolls are fixed in space and the basic wave-number is assigned, *a priori*. The interesting questions which arise because of three-dimensionality and consequent possible phase shifts of the convecting pattern are beyond the scope of this work. However, within the limitations of the approach we can answer a variety of questions.

The method of solution is set up so as to enable us to derive dependable results for Rayleigh numbers, R, up to 30 times the critical Rayleigh number, R_c (the latter being defined as the minimum value at which the system is unstable to infinitesimal perturbations). Hence, we deduce information about the heat flux and the structure of the temperature and velocity fields for highly non-linear flows. The calculations are compared with those derived by previous investigators and, since we can impose confidence limits on the present results, a comparison can be made between the techniques of this paper and those of earlier workers.

The solutions are carried out for Prandtl numbers ranging over more than four orders of magnitude so that we can test the dependence of heat flux and other properties of the system on Prandtl number. At fixed values of the Rayleigh number and the Prandtl number we also calculate the heat flux as a function of wave-number.

2. The mathematical system

The lower boundary ($z = 0$) of the fluid is maintained at temperature T_0 and the temperature of the upper boundary ($z = d$) is $T_0 - \Delta T$. We write the total temperature as

$$T_{\text{total}} = T_0 - \Delta T z/d + T(x, z, t). \tag{2.1}$$

In (2.1) the final term represents the deviations of the temperature from the linear (conductive) profile.

The equations (all variations with respect to y are assumed to vanish) are the two-dimensional Boussinesq equations for the conservation of momentum,

$$\partial \mathbf{v}/\partial t + \mathbf{v}.\nabla \mathbf{v} = -\rho_0^{-1} \nabla p - g(\mathbf{k}\rho'/\rho_0) + \nu \nabla^2 \mathbf{v}, \tag{2.2}$$

the conservation of mass,

$$\partial u/\partial x + \partial w/\partial z = 0, \tag{2.3}$$

the linear equation of state for the fluctuating density,

$$\rho'/\rho_0 = -\alpha T' \tag{2.4}$$

and the equation for the conservation of heat,

$$\partial T/\partial t - w\Delta T/d + \mathbf{v}.\nabla T = \kappa \nabla^2 T. \tag{2.5}$$

Here, $\mathbf{v}$ is the two-dimensional velocity vector with components (u, w) in the respective directions (x, z); g is the gravitational acceleration in the negative z-direction; ρ_0 is the density at temperature T_0; α is the coefficient of thermal expansion; and ν and κ are respectively the coefficients of kinematic viscosity and thermometric diffusivity. In equation (2.5) the linear part of T_{total} has been separated out and appears as the second term.

Cross-differentiating the first and third equations of motion in order to eliminate the pressure, p, and defining the y-component of vorticity as

$$\eta = \partial u/\partial z - \partial w/\partial x, \tag{2.6}$$

we have

$$\partial \eta/\partial t + \mathbf{v}.\nabla \eta = -g\alpha \partial T/\partial x + \nu \nabla^2 \eta. \tag{2.7}$$

We introduce the stream function, ψ, through the definitions

$$u = \partial \psi/\partial z, \quad w = -\partial \psi/\partial x \tag{2.8}$$

so that

$$\eta = \nabla^2 \psi. \tag{2.9}$$

Our system then becomes

$$\partial \eta/\partial t = J(\psi, \eta) - g\alpha \partial T/\partial x + \nu \nabla^2 \eta, \tag{2.10}$$

$$\partial T/\partial t = J(\psi, T) - d^{-1}\Delta T\, \partial \psi/\partial x + \kappa \nabla^2 T. \tag{2.11}$$

Finally we non-dimensionalize the system by means of the definitions†

$$\mathbf{v} = \kappa d^{-1}\mathbf{v}', \quad t = d^2\kappa^{-1}t', \quad (x, z) = d(x', z'), \quad T' = T/\Delta T, \tag{2.12}$$

where the primed quantities are non-dimensional. Then equations (2.10) and (2.11) become

$$\partial \eta/\partial t = J(\psi, \eta) - \sigma R\, \partial T/\partial x + \sigma \nabla^2 \eta, \tag{2.13}$$

$$\partial T/\partial t = J(\psi, T) - \partial \psi/\partial x + \nabla^2 T, \tag{2.14}$$

where all of the variables are non-dimensional, the primes have been dropped and the following non-dimensional parameters appear:

$$\left.\begin{aligned} &\text{Prandtl number:} \quad \sigma = \nu/\kappa, \\ &\text{Rayleigh number:} \quad R = g\alpha \Delta T d^3/\kappa\nu. \end{aligned}\right\} \tag{2.15}$$

The boundary conditions are based on the assumptions that the boundaries, $z = 0$, $z = 1$, are perfect conductors of heat and are flat and stress-free. Then the conditions are

$$\psi = 0, \quad \partial^2 \psi/\partial z^2 = 0, \quad T = 0, \quad \text{on} \quad z = 0, 1. \tag{2.16}$$

† The manner of non-dimensionalizing the equations is arbitrary and is not important unless one wishes to use the non-dimensional system either for making order of magnitude arguments about the variables or for trying to conjecture about the magnitudes of the various terms. We merely point out here that with the present scheme for Bénard convection the variables show very little change when the Prandtl number is varied over more than four orders of magnitude. However, the stream function and, consequently, the velocities show a strong dependence on the Rayleigh number as would be expected.

When rigid boundary conditions are chosen, the second condition becomes

$$\partial\psi/\partial z = 0. \tag{2.17}$$

However, in this case the method of expansion in the following section is too cumbersome and a different technique must be used.

3. Expansion in terms of eigenmodes

In accord with the remarks in the introduction we assume that the evolved motion field after instability has the form of two-dimensional rolls, independent of the y-direction and with a basic horizontal wave-number denoted by α. Then a general spatial representation which satisfies the boundary conditions is

$$\left.\begin{aligned}\psi &= \sum_{m=1}^{M}\sum_{n=1}^{N} a_{mn}\sin m\pi\alpha x\sin n\pi z,\\ T &= \sum_{m=0}^{M}\sum_{n=1}^{N} b_{mn}\cos m\pi\alpha x\sin n\pi z,\end{aligned}\right\} \tag{3.1}$$

where the a_{mn} and b_{mn} are generally functions of time. This representation, in fact, is composed of the eigenfunctions of the linear stability problem and if M and N are allowed to become infinite the representation is a complete orthogonal set. In our treatment we shall truncate the representation by choosing finite values of M and N so that the representation will be only approximate. The accuracy of the method of solution is discussed in connexion with specific solutions which are presented in § 5.

If expressions (3.1) are substituted into equations (2.13) and (2.14) and if we multiply these equations respectively by $\sin p\pi\alpha x\sin q\pi z$, and $\cos p\pi\alpha x\sin q\pi z$ and integrate the equations from $x = 0$ to $x = 1/\alpha$ and $z = 0$ to $z = 1$, we derive a set of non-linear ordinary, differential (in time), equations for the amplitudes of the harmonic components. These are

$$\begin{aligned}\dot{a}_{pq} = &-\sigma\pi^2(p^2\alpha^2+q^2)a_{pq} - \frac{\sigma R\alpha p}{\pi(p^2\alpha^2+q^2)}b_{pq}\\
&+\frac{\pi^2\alpha}{4(p^2\alpha^2+q^2)}\left\{\sum_{m=1}^{p-1}\sum_{n=1}^{q-1}(mq-np)[(p-m)^2\alpha^2+(q-n)^2]a_{mn}a_{p-m,q-n}\right.\\
&+\sum_{m=p+1}^{M}\sum_{n=q+1}^{N}(mq-np)[(p-m)^2\alpha^2+(q-n)^2-(m^2\alpha^2+n^2)]a_{m-p,n-q}a_{mn}\\
&+\sum_{m=p+1}^{M}\sum_{n=1}^{q-1}[p(n-q)+mq][m^2\alpha^2+(q-n)^2]a_{m-p,n}a_{m,q-n}\\
&+\sum_{m=p+1}^{M}\sum_{n=q+1}^{N}[q(m-p)+np][(m-p)^2\alpha^2+n^2-(m^2\alpha^2+(n-q)^2)]a_{m,n-q}a_{m-p,n}\\
&+\sum_{m=p+1}^{M}\sum_{n=1}^{q-1}(np-mq)[(m-p)^2\alpha^2+(q-n)^2]a_{mn}a_{m-p,q-n}\\
&+\sum_{m=1}^{p-1}\sum_{n=q+1}^{N}[p(q-n)-mq][(p-m)^2a^2+n^2]a_{m,n-q}a_{p-m,n}\\
&\left.+\sum_{m=1}^{p-1}\sum_{n=q+1}^{N}(np-mq)[(p-m)^2\alpha^2+(n-q)^2]a_{mn}a_{p-m,n-q}\right\},\end{aligned} \tag{3.2}$$

$$\dot{b}_{pq} = -\pi^2(p^2\alpha^2+q^2)b_{pq} - \pi\alpha p a_{pq}$$
$$+\delta\frac{\pi^2\alpha}{4}\Bigg\{\sum_{m=0}^{p-1}\sum_{n=1}^{q-1}(np-mq)a_{p-m,q-n}b_{mn} + \sum_{m=p}^{M}\sum_{n=q+1}^{N}(np-mq)a_{nm}b_{m-p,n-q}$$
$$+\sum_{m=p+1}^{M}\sum_{n=q+1}^{N}[p(q-n)-mq]a_{m-p,n}b_{m,n-q} + \sum_{m=p}^{M}\sum_{n=q+1}^{N}[p(q-n)-mq]a_{m,n-q}b_{m-p,n}$$
$$+\sum_{m=p+1}^{M}\sum_{n=q+1}^{N}(np-mq)a_{m-p,n-q}b_{mn} + \sum_{m=0}^{p-1}\sum_{n=q+1}^{N}[p(n-q)+mq]a_{p-m,n}b_{m,n-q}$$
$$+\sum_{m=0}^{p-1}\sum_{n=q+1}^{N}(mq-np)a_{p-m,n-q}b_{mn} + \sum_{m=p}^{M}\sum_{n=1}^{q-1}[q(m-p)+np]a_{m,q-n}b_{m-p,n}$$
$$+\sum_{m=p+1}^{M}\sum_{n=1}^{q-1}(mq-np)a_{m-p,q-n}b_{mn}\Bigg\}, \tag{3.3}$$

where $0 \leqslant p \leqslant M$, $1 \leqslant q \leqslant N$ and $\delta = \frac{1}{2}$ when $p = 0$ in (3.3) otherwise $\delta = 1$. The superdot on the left side of each equation corresponds to a time derivative.

These equations must be integrated in time so that a suitable set of initial conditions must be given. Generally for a given value of σ and a supercritical value of R an arbitrary disturbance is introduced initially. The problem is to find the behaviour of the harmonic amplitudes as functions of time. For $M = 2, N = 2$, steady analytic solutions have been found for special values of the non-dimensional parameters (Veronis 1965*a*, 1966). For larger values of M and N no analytic solutions have been found and it has been necessary to integrate the equations numerically. The procedure is described in the following section.

4. Method of solution

When M and N are larger than 2, the system of equations becomes very cumbersome. However, with electronic computers it is possible to treat fairly extensive systems of this type.

The specific approach taken here is the following: We choose a maximum total wave-number, K. By 'maximum total wave-number' we mean that the sum of the x and z wave-numbers cannot exceed K, i.e. $p+q \leqslant K$ or $m+n \leqslant K$. We then follow the behaviour of all components whose total wave-number is K or less. In the largest system analysed, K was chosen to be 10 so that all modes of behaviour with $p+q \leqslant 10$ were allowed. We show the representation as modal combinations (m, n) in figure 1. The present type of truncation was chosen because it turns out that only alternate diagonals contain non-vanishing modes (shown by crosses in the lattice of figure 1). In particular, with the type of symmetry that exists for the present problem all modes such that $m+n$ is an odd number vanish. Hence, by taking into account alternate diagonals we have an efficient manner of treating all non-vanishing modes up to a given order. A square array is less efficient. For example, a problem was solved with all the terms in the square array $m \leqslant 3, n \leqslant 3$. It turned out that the component $m = 3$, $n = 3$ vanished. But the latter does not vanish when other components with $m+n = 6$ are taken into account.

Because of the excessive length of the equations for a system as large as that which occurs for $K = 10$, special computer programs were required to make it possible to generate the non-linear terms in a form which could be used directly by

the computer. The type of programming which was used is reported elsewhere (Veronis 1965*b*). We note here that with $K = 10$ the heat equation is represented by 30 component equations with a total of approximately 1500 non-linear terms. The vorticity equation contains fewer terms.

When two total wave-numbers interact and produce a total wave-number larger than K the interaction is ignored as are all interactions which involve wave-numbers larger than K but which produce wave-numbers smaller than K. Hence the present

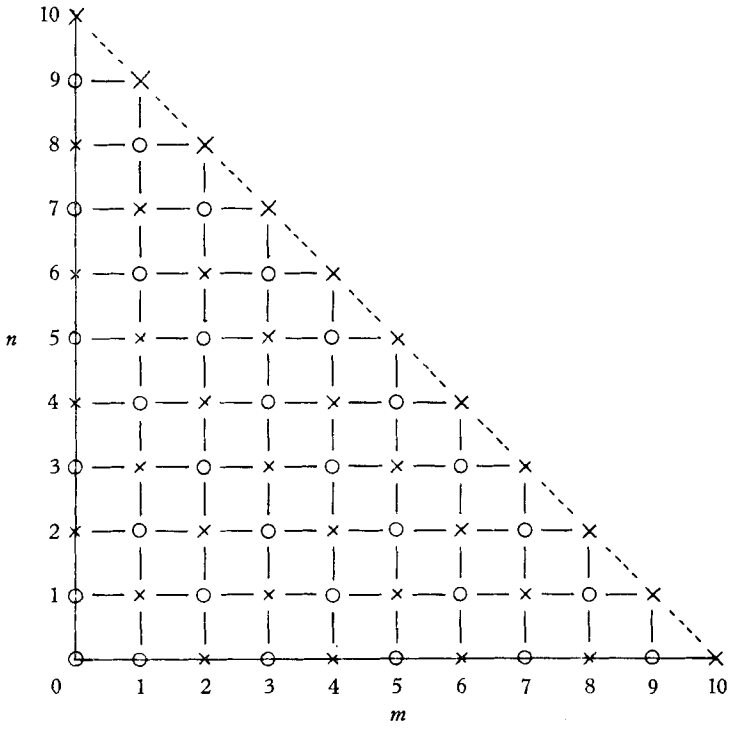

FIGURE 1. The lattice of modal combinations (m, n) which are taken into account in the calculations. Modes marked with a cross ($m+n$ = even number) contribute to the behaviour of the system whereas those marked with a small circle ($m+n$ = odd number) decay and were left out of the calculation after a few runs showed this decay. The diagonal line running from upper left to lower right determines the size of the systems which are treated. All modes included between the axis and a diagonal line are included in a single run.

method of solution is qualitatively similar to an expansion in terms of a small parameter because in both methods interactions up to a certain order only are allowed. However, the present technique does not involve a linearization procedure and the results are presumably more complete than those from a perturbation method.

The equations have been integrated numerically, using an implicit time integration scheme; i.e. the time derivative in equations (3.2) and (3.3) were evaluated at the centres of the time intervals.

5. Results of calculations

A number of time integrations of the equations for simple Bénard convection was made using the method described in the foregoing sections. The results are described in the several subsections which follow. First we note how the results are presented.

For Bénard convection the minimum value, R_c, of the Rayleigh number at which instability to infinitesimal disturbances occurs is equal to $27\pi^4/4 = 657{\cdot}5$ when the boundaries are free or slippery. The horizontal scale of the motion at this value of R_c is given by $\alpha^2 = 0{\cdot}5$.

The Nusselt number, Nu, is defined as the ratio of the vertical heat flux, H, to the conductive vertical heat flux per unit horizontal area. In the steady state the vertical heat flux must be independent of the vertical co-ordinate, z, and can therefore be evaluated by the heat flux through the lower boundary, $z = 0$. Thus

$$H = -\kappa \left\langle \frac{\partial}{\partial z} T_{\text{total}} \right\rangle_{z=0}, \tag{5.1}$$

where the angular brackets correspond to a horizontal average. With equation (3.1) for T, equation (5.1) can be written as

$$H = \kappa \frac{\Delta T}{d} - \kappa \frac{\Delta T}{d} \sum_{n=1}^{N} n\pi b_{0n}. \tag{5.2}$$

Hence, the Nusselt number is given by

$$Nu = \frac{Hd}{\kappa \Delta T} = 1 - \pi \sum_{n=1}^{N} n b_{0n}. \tag{5.3}$$

We present our results as plots or tables of Nusselt number *vs.* R/R_c, the ratio of the Rayleigh number to the critical value when $\alpha^2 = 0{\cdot}5$.

(*a*) *Accuracy of solutions*

In the integration of the equations the system invariably settled down to a steady state. The criterion for convergence was taken as

$$|f^{\tau+1} - f^{\tau}| < 0{\cdot}0001, \tag{5.4}$$

where f represents each Fourier amplitude at time $t = \tau \Delta t$. It would have been preferable to incorporate the time increment, Δt, into the criterion but that was not done for this set of runs. Hence, cases with larger values of Δt were required to satisfy a more stringent criterion than those with smaller Δt. However, the results were found to be accurate to three and, in many cases, four significant digits when different values of Δt were used for the same run. Hence, we can rely on three significant digits for the amplitudes of the Fourier components and for the heat flux. In some of the runs where R was held fixed for different values of the Prandtl number we present four significant digits where the differences are small.

(*b*) *Validity of the results*

A measure of the validity of the results is given by the degree of agreement between runs with different values of K, the maximum wave-number in the representation. It turned out that the reliability of the values of heat flux as a function of K

depended on the values of the Rayleigh number (not surprising) and the Prandtl number. In general, larger values of R required a larger representation as would be expected. Also, smaller values of σ required a larger representation.

In table 1 we list the steady-state values of Nu as a function of R for $K = 2, 6, 8, 10$ for $\sigma = 6{\cdot}8$ (corresponding to water) with $\alpha^2 = 0{\cdot}5$. The case $K = 2$ is a special one since it is independent of σ. The relation between Nusselt number and Rayleigh number for $K = 2$ can easily be derived analytically and is

$$H = 3 - 2R_c/R. \tag{5.5}$$

Hence, values of Nu for $K = 2$ are listed in the right-hand column and apply to all values of σ.

R/R_c	$K = 6$	$K = 8$	$K = 10$	$K = 2$
1	1	1	1	1
1·1	1·18	1·18	1·18	1·18
1·2	1·34	1·34	1·34	1·33
1·4	1·61	1·61	1·61	1·57
2	2·14	2·14	2·14	2·00
3	2·68	2·68	2·68	2·33
4	3·04	3·04	3·04	2·50
6	3·55	3·55	3·55	2·67
8	3·92	3·93	3·93	2·75
10	4·22	4·24	4·24	2·80
15	4·76	4·84	4·85	2·87
20	5·13	5·30	5·33	2·90
30	5·61	5·99	6·08	2·93
40	5·91	6·49	6·68	2·95
50	6·11	6·86	7·16	2·96

K corresponds to the size of the system or the total wave-number (cf. § 4).

TABLE 1. Nu *vs.* R/R_c for $\sigma = 6{\cdot}8$

For the case of water ($\sigma = 6{\cdot}8$) we see that the representation given by $K = 6$ gives results for Nu identical (to three significant digits) with the results given by the better representations $K = 8$ and $K = 10$ when $R \leqslant 6R_c$. Even at $R = 10R_c$ the discrepancy is very small ($< \frac{1}{2}\%$) but above $10R_c$ the values of Nu for $K = 6$ fall below those given by $K = 8$ and $K = 10$. *We shall accept results which agree to within* 1 % *of those of the next higher approximation.* Hence at $R = 20R_c$ we accept the Nusselt number given by $K = 8$. Even at $30R_c$ the $K = 8$ result differs from that using $K = 10$ by only 1·5 %. Hence, the value for $K = 10$ very likely satisfies the above criterion of acceptability because an increased representation always results in a sharp decrease in the discrepancy (note, for example, the values for $R = 40R_c$ and $R = 50R_c$ for $K = 6$, 8 and 10).

We shall investigate the dependence of Nu on σ shortly. However, for our present purposes it is worth our while to note that for $\sigma < 0{\cdot}025$ and at $R = 20R_c$ the representations $K = 8$ and $K = 10$ yield values of Nu which differ more and more with decreasing σ. At $R = 15R_c$ the results for $K = 8$ agree with those for $K = 10$ for $\sigma \geqslant 0{\cdot}005$.

Heat flux is an integral property of the system and therefore provides only the crudest check on consistency of solutions for different values of K. We shall also look at the mean temperature profile in the vertical in a later subsection and can use the consistency of this spatial variation of a property as an additional measure of validity of results.

(c) *Heat flux as a function of Rayleigh number*

The dependence of Nu on R will be discussed for $\sigma = 6{\cdot}8$. Other values of σ yield qualitatively similar results. Quantitative differences are discussed later.

The system with $K = 2$ yields values of Nu identical with those obtained from second-order perturbation theory (Malkus & Veronis 1958). It is seen from table 1

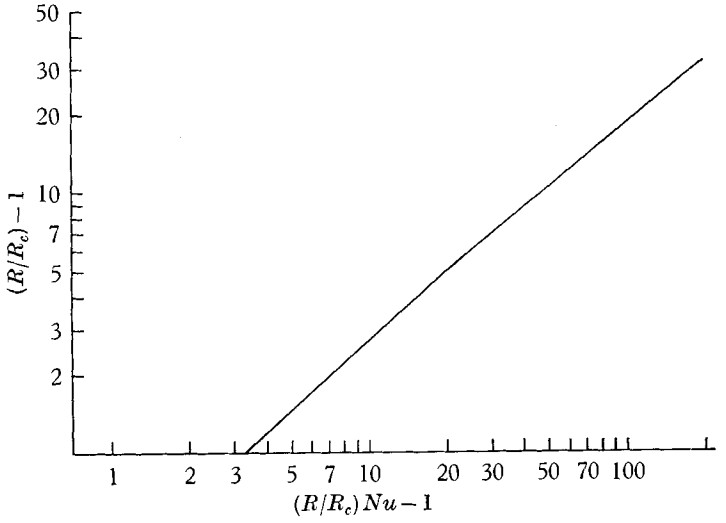

FIGURE 2. Plot of $\log([R/R_c]Nu-1)$ *vs.* $\log(R/R_c-1)$ in the range $2R_c \leqslant R \leqslant 30R_c$. The two line segments give the values 1·15 and 1·26 for the power laws in the ranges $2R_c \leqslant R < 6R_c$, $6R_c < R \leqslant 30R_c$.

that this representation is adequate only for values of R very close to the critical value. For $R > 2R_c$ the heat flux is seriously underestimated by this limited representation.

In figure 2 we show the values of the convective heat flux $([R/R_c]Nu-1)$ as a function of $(R/R_c)-1$ on log–log paper and as given by the representation $K = 10$. We have already noted that for the range $R \leqslant 20R_c$ this representation gives reliable results. In the range $R > 6R_c$ the points lie very nearly along the straight line whose slope is determined by the relation

$$\log\left(\frac{R}{R_c}Nu-1\right) = \text{const.} \times \log\left(\frac{R}{R_c}-1\right)^{1{\cdot}26}. \tag{5.6}$$

This agrees almost exactly with Jakob's (1949) experimental results where $\log([R/R_c]Nu) \sim \log(R/R_c)^{1{\cdot}25}$ for Rayleigh numbers in this range. For $2R_c < R < 6R_c$ the slope is approximately 1·15 instead of 1·26.

(*d*) *Heat flux as a function of Prandtl number*

Results have been derived for $R \leqslant 20R_c$ and $100 \leqslant \sigma \leqslant 0{\cdot}005$. For small values of the Rayleigh number the heat flux is insensitive to large changes in σ. In the steady state the Prandtl number enters explicitly only through the non-linear momentum terms and these vanish when $K = 2$. For larger representations the inertial terms have a contribution but this was found to be negligible at low Rayleigh number for $\sigma \geqslant 0{\cdot}005$.

As the Rayleigh number is increased the heat flux has been found to depend weakly on Prandtl number. The general dependence is as follows. For the Rayleigh numbers, $R = 6$, 10, 15, 20, the heat flux is slightly larger (but negligibly so) at

σ ...	100	6·8	4	2	1	0·1	0·025	0·01	0·005
$R = 6R_c$ $K = 8$	3·554	3·553	—	—	3·58	3·61	3·612	3·614	3·614
$R = 10R_c$ $K = 8$	4·244	4·241	—	—	4·38	4·388	4·390	4·393	4·394
$R = 15R_c$ $K = 10$	4·85	4·85	4·89	4·99	5·06	5·109	5·113	5·114	5·114
$R = 20R_c$ $K = 10$	5·33	5·33	—	—	5·62	5·670	5·675	5·676	5·676

All calculations agree with those of the next lower order in K to within 0·5 % except for the values at $R = 20R_c$, where $K = 10$ has been used. With the present scheme it was not possible to go beyond $K = 10$.

TABLE 2. Nusselt number as a function of Prandtl number

$\sigma = 100$ than it is at $\sigma = 6{\cdot}8$. A relatively sharp increase in heat flux occurs between $\sigma = 6{\cdot}8$ and $\sigma = 1$. For the range $1 \geqslant \sigma \geqslant 0{\cdot}01$ the heat flux rises slowly but monotonically, and seems to settle down when $\sigma \leqslant 0{\cdot}01$. The size of the increase in Nu between $\sigma = 100$ and $\sigma = 0{\cdot}005$ depends on the Rayleigh number, being greater for larger R. Thus at $R = 20R_c$ the increase is approximately 7 %, whereas for $R = 6R_c$ the increase is less than 2 %. However, the monotonic character of the change is unmistakeable as can be seen in table 2, where we have summarized the results.

At $R = 6R_c$ the system is adequately described by $K = 6$ but we show $Nu vs. \sigma$ using $K = 8$. At $R = 10R_c$ the values of Nu using $K = 8$ agree with those at $K = 10$. For $R = 15R_c$ and $R = 20R_c$ we show the results for $K = 10$. The latter case exhibits the same qualitative dependence of Nu on R as did the other cases but it should be pointed out that the values of Nu for $\sigma = 0{\cdot}025$, $\sigma = 0{\cdot}01$ and $\sigma = 0{\cdot}005$ differ by as much as 4 % from the values given by $K = 8$. We noted earlier that the smaller the σ the larger the representation required at a given Rayleigh number to give acceptable results and the results at $R = 20R_c$ reflect this point strongly. We shall return to a discussion of the representation in the next subsection. It suffices here to note that at $R = 20R_c$ the qualitative behaviour of $Nu vs. \sigma$ is the same as at lower Rayleigh numbers.

Why does the heat flux increase with decreasing Prandtl number? It is difficult to give a general argument from the equations themselves because the equations can be non-dimensionalized in several ways so that σ appears in different places;

moreover, the dependence on σ seems to be an implicit one. As σ is decreased, the magnitude of the temperature fluctuations decreases slightly but the velocities increase so that the change in the mean temperature maintains the same magnitude. Furthermore, as we shall see in the next subsection, at a fixed Rayleigh number the scale of the smallest significant disturbance decreases with decreasing σ. Hence, any general argument which attempts to explain the present result must take into account some aspects of the structure of the system.

The Prandtl number can be used as a measure of the relative significance of the inertial terms in the equations of motion to the convective terms in the heat equation or, alternatively, as a relative measure of diffusion of momentum to diffusion of temperature. Large values of σ imply that the inertial terms in the heat equation are negligible and that the important processes which contribute to an out-of-phase relation between temperature and velocity fields occur in the heat balance through the convection terms. Small values of σ emphasize the out-of-phase effects of the inertial terms in the momentum equations. From our present findings we note that smaller heat flux at larger σ indicates that the out-of-phaseness introduced by fluctuating interactions of temperature and velocity fields appear to be more destructive to efficient transfer of heat than are corresponding effects of inertial terms. Of course, this speculation is dependent on the dynamics of this particular problem. It is possible that the presence of rigid boundaries or the onset of three-dimensional motions would change the characteristic behaviour.

(*e*) *The spatial dependence of temperature and velocity*

Figures 3(*a*) and 3(*b*) exhibit the spatial dependence (for half-cells) of ψ and $(T_{\text{total}}-T_0)/\Delta T$ for the case $\sigma = 6{\cdot}8$ and $R = 20R_c$. We use the representation $K = 10$ for these graphs since it is adequate to represent the physical system. The contour lines for the stream function show that the motion field contains the basic harmonic with a slight distortion provided by the higher harmonics. Thus the motion consists of a single overturning cell carrying warm fluid upward and cold fluid downward. The temperature field exhibits characteristic features for large values of R, viz. a large mass of nearly isothermal fluid in the centre of the cell and mushroom-shaped isotherms. Thus warm fluid is carried from the lower regions toward the upper regions and is squashed up close to the upper boundary where diffusive processes remove the heat from the fluid.

Figures 4(*a*) and 4(*b*) show the non-dimensional mean temperature,

$$-z+\sum_{n=1}^{N} b_{0n}\sin n\pi z,$$

as a function of the vertical co-ordinate, z, for the values $R = 2, 4, 6, 8, 15, 20$ when $\sigma = 6{\cdot}8$ and $\sigma = 0{\cdot}025$ respectively. It is evident that, as R is increased, a thick region in the centre of the fluid achieves a nearly isothermal state in the mean. The thickness of the isothermal region increases with increasing R.

An unmistakeable positive vertical temperature gradient or reversal of temperature occurs in the fluid. This has been found to be present for all values of σ. Thus, it appears that the fluid creates a refrigeration region; i.e., even though the system is heated from below and cooled from above, in the centre band cooler fluid underlies

warmer fluid. This result is contrary to one's (or at least the author's) intuition. It should be noted that the amplitude of the positive gradient is small. The temperature overshoots the mean value of the fluid by about 6 % of the total temperature drop across the layer. As the Rayleigh number is increased, the region about the middle

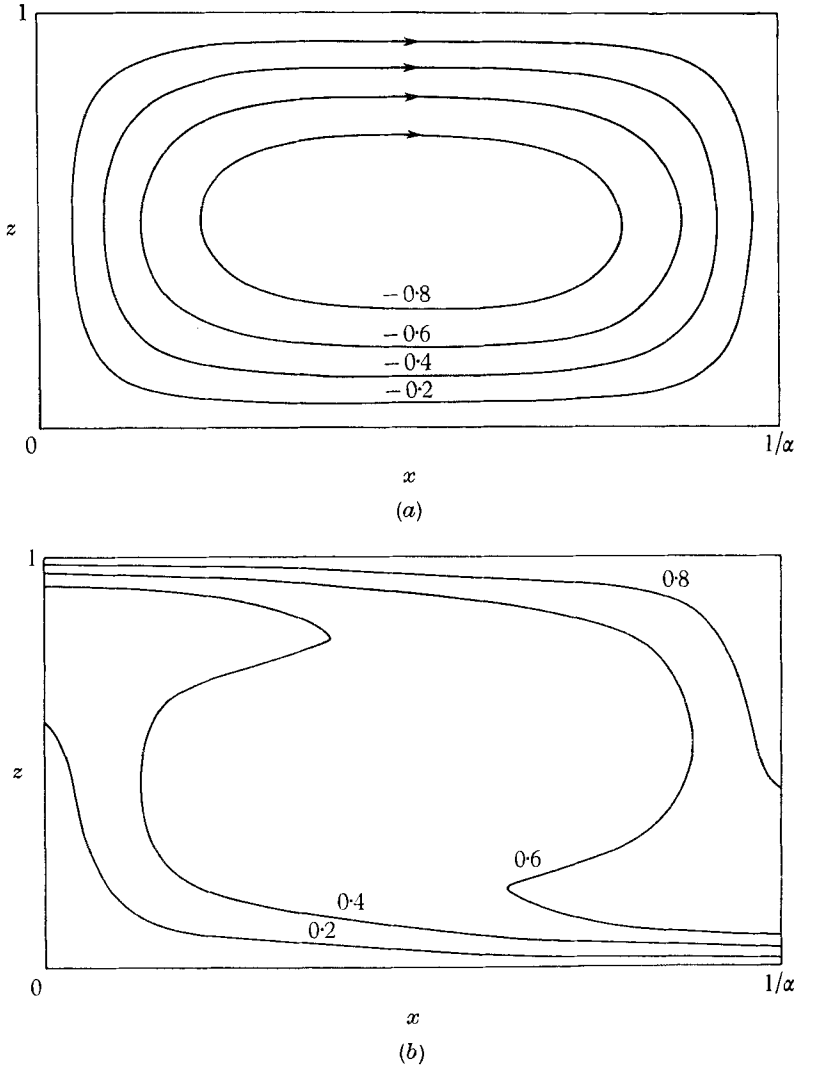

FIGURE 3. Contour lines of ψ in (*a*) and $(T_{\text{total}}-T_0)/\Delta T$ in (*b*) in the range $0 \leqslant x \leqslant 1/\alpha$, $0 \leqslant z \leqslant 1$ for the case $\sigma = 6{\cdot}8$ and $R = 20R_c$ from the representation $K = 10$.

of the layer becomes more nearly isothermal with small kinks of overshoot before the band joins to the sharp gradient region near the boundary.

Another point worth noting is that smaller values of σ are accompanied by slightly smaller temperature fluctuations but correspondingly larger velocities. Hence, the mean temperature profile is as distorted from the linear profile for small σ as it is for larger σ.

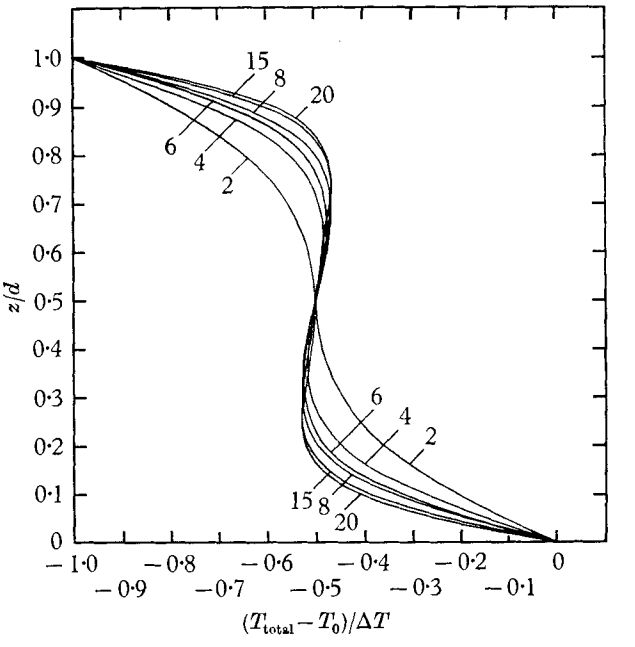

(*a*)

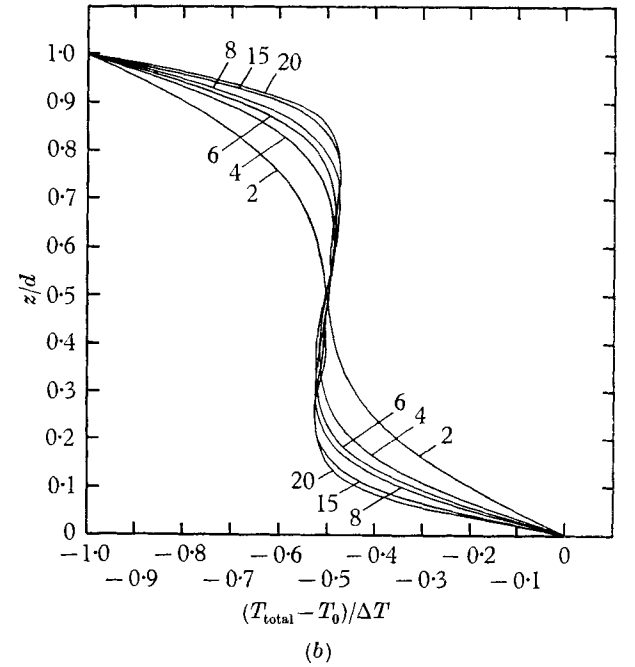

(*b*)

FIGURE 4. The mean temperature, $\langle T_{\text{total}}-T_0\rangle/\Delta T$ as a function of z for the cases $R = 2, 4, 6, 8, 15, 20$ when $\sigma = 6{\cdot}8$ in (*a*) and $\sigma = 0{\cdot}025$ in (*b*). The nearly isothermal region in the centre band increases in thickness as R increases. The small negative gradients noted in the text are evident for $R \geqslant 4$.

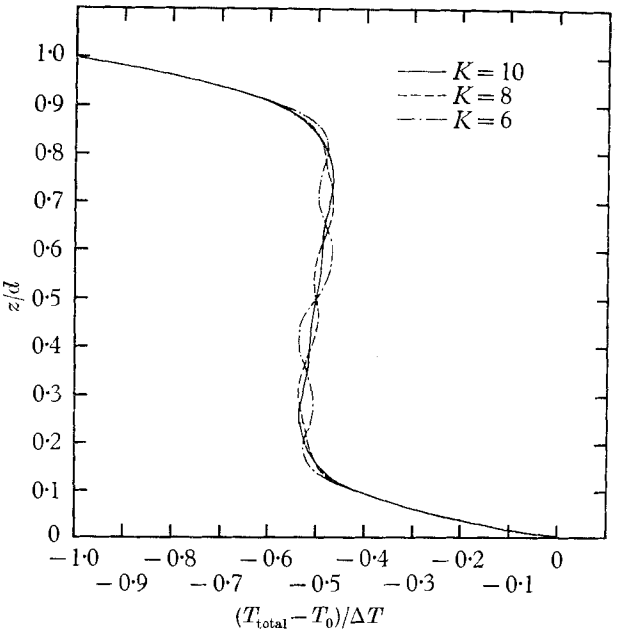

(*a*)

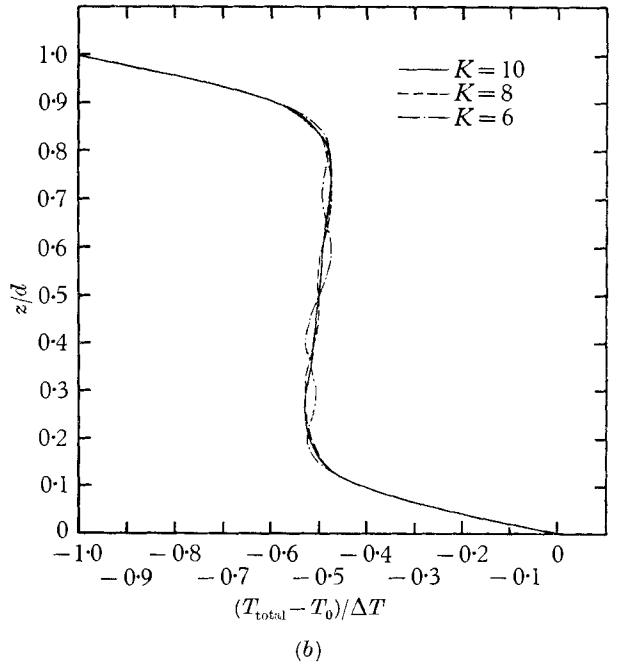

(*b*)

FIGURE 5. The vertical profile of the mean temperature with the three representations $K = 6$, 8, and 10 for the cases $\sigma = 6{\cdot}8$, $R = 20R_c$ in (*a*), and $\sigma = 0{\cdot}025$, $R = 15R_c$ in (*b*). The agreement of successive approximations is a measure of the validity of the representation.

We have discussed the validity of the results at different points in the foregoing discussion. The convergence of the successive approximations to the real steady-state value may be seen with more clarity in figure 5, where we have plotted the mean temperature *vs.* the vertical co-ordinate. In figure 5(*a*) we exhibit such graphs for the case $\sigma = 6{\cdot}8$, $R = 20R_c$ with $K = 6$, 8 and 10. It is clear that the representation $K = 6$ is definitely inadequate. However, the cases $K = 8$ and $K = 10$ nearly coincide so that one has considerable confidence that the results are acceptable in describing the system.

For $\sigma = 0{\cdot}025$ the curves are nearly the same as for $\sigma = 6{\cdot}8$. In this case, the system $K = 6$ deviates further from the $K = 10$ system than in the previous example. Also, because the representations $K = 8$ and $K = 10$ give results which differ a bit more, one cannot conclude from such a comparison that the latter is a good description of the system. However, the curve for $K = 10$ does exhibit the

	σ					
α	100	6·8	1	0·2	0·1	0·025
$2^{-\frac{1}{2}}$	4·22	4·22	4·31	4·34	—	4·345
0·75	—	4·235	4·32	4·35	—	4·36
0·8	4·24	4·24	4·32	4·350	4·36	4·36
0·85	4·24	4·23	4·30	4·34	—	4·35
0·9	4·23	4·22	4·27	4·31	4·315	4·32

TABLE 3. Values of Nu at $R = 10R_c$ as a function of α and σ

same characteristic behaviour as is seen in other cases where the results differ from those with $K = 8$ by a negligible amount. For example, the mid-region is very nearly isothermal and there is no evidence of more than one reversal of temperature up to the midpoint of the fluid. It is for this reason that we have made use of the results for $\sigma = 0{\cdot}025$, $R = 20R_c$ in our earlier discussion.

When the Rayleigh number is dropped to $15R_c$ with $\sigma = 0{\cdot}025$ the cases $K = 8$ and $K = 10$ agree quite well as can be seen in figure 5*b*.

From the foregoing results we see that keeping the Rayleigh number fixed and decreasing the Prandtl number means that a larger representation is required to describe the system. Thus, smaller scale motions are evidently generated at smaller values of σ and the dependence on Prandtl number is reflected in the internal, detailed structure of the motion and temperature fields. Strong dependence on σ should manifest itself more in the rigid boundary case where motion must satisfy a non-slip condition and a viscous boundary layer must necessarily exist.

(*f*) *Heat flux as a function of wave-number*

A set of runs was made to determine the Nusselt number as a function of wave-number, α, at $R = 10R_c$ for several different values of σ. The results with the representation $K = 6$ are summarized in table 3. With $K = 6$ there is an uncertainty in the absolute values of Nu which is greater than the differences between the Nu values at different α. However, for a relative comparison the figures suffice. We note that for this relatively small value of R the wave-number at which maximum

heat flux occurs lies between $\alpha = 0{\cdot}75$ and $\alpha = 0{\cdot}8$ and therefore is somewhat larger than the critical wave-number at marginal instability. Herring (1963) found a much stronger dependence at very large Rayleigh numbers.

The heat flux as a function of Prandtl number also changes as a function of α. At $\alpha = 0{\cdot}9$ there is less dependence on σ than there is at $\alpha = \sqrt{2}/2$ since Nu has increased slightly at $\sigma = 100$ and decreased at $\sigma = 0{\cdot}025$. Thus the range of Nu has been decreased.

6. Comparison with previous calculations

The present calculations are valid over a much larger range of Rayleigh number than those of Malkus & Veronis (1958). The latter expanded the variables in terms of a parameter which was effectively $(R/R_c - 1)^{\frac{1}{2}}$ and the sixth-order results which were derived (p. 239) were assumed valid in the range below $3R_c$. The present results show that the previous calculations were, in fact, valid only for $R \leqslant 2R_c$.

Kuo's (1961) calculations of the steady system were based on the expansion parameter $\eta = (1 - R_c/R)^{\frac{1}{2}}$ and his results checked in successive approximations over a range extending to $8R_c$. His method differs from the present one in two respects. He used a perturbation parameter and we do not. Also, the specific terms which he retained were determined by his ordering procedure, whereas in our case we simply take into account all terms up to a given total wave-number. We rely on the reproducibility of results through successively higher representations as a check on convergence and Kuo used essentially the same criterion. The Nusselt numbers from the two calculations (Kuo used $\sigma = 10$ and our results are for $\sigma = 6{\cdot}8$, but the system is insensitive to the change in σ at these small Rayleigh numbers) are compared below:

	R/R_c ...	2	3	4	6	8
Kuo's	Nu	2·14	2·66	3·02	3·50	3·85
Ours	Nu	2·14	2·68	3·04	3·55	3·93

We have used Kuo's values as computed from his $S^{(4)}$. The results given by $S^{(d)}$ in his paper involve a mixing of orders and turn out to be 8 % higher at $R = 8R_c$ than the calculations in this paper.

Kuo derived an exponent of 1·19 in the relation between heat flux ($S^{(4)}$) and Rayleigh number. This is probably due to the fact that he measured the slope for $R \leqslant 8R_c$ and in that range a single straight line on the log–log plot would give something between our values of 1·15 for $R < 6R_c$ and 1·26 for $R > 6R_c$.

Our results and Kuo's, therefore, agree quite well in the range of overlap. This agreement indicates that his expansion procedure is sound for $R > R_c$. When motions can occur for $R < R_c$ (finite amplitude instability) his expansion parameter is probably less useful since it can exceed unity and the question of the radius of convergence is raised. The mixing of terms involved in his derivation of $S^{(d)}$ values is probably also unacceptable as a good measure of the heat flux. Kuo presented the $S^{(d)}$ values as a possibly better approximation but he had no recourse to a more exact answer for comparison at larger values of R. It is, however, remarkable that his method of solution using an expansion procedure should give the precision that it does at values of R so far above the critical value.

In his discussion of the mean temperature profile Kuo points out that a broad band of fluid centred about the middle of the layer is isothermal. Our results show that this mid-region is nearly isothermal but has a slightly stable gradient. Kuo's figure also shows this feature although he does not mention it in his discussion.

Herring (1963) has calculated the heat flux for a model in which all non-linear interactions which do not involve, or contribute to, the mean temperature field are omitted. The calculations are independent of σ since his system of equations does not involve σ. His results up to $15R_c$ are shown in figure 6 together with those from the present calculations for water and mercury. It is evident that the omission of

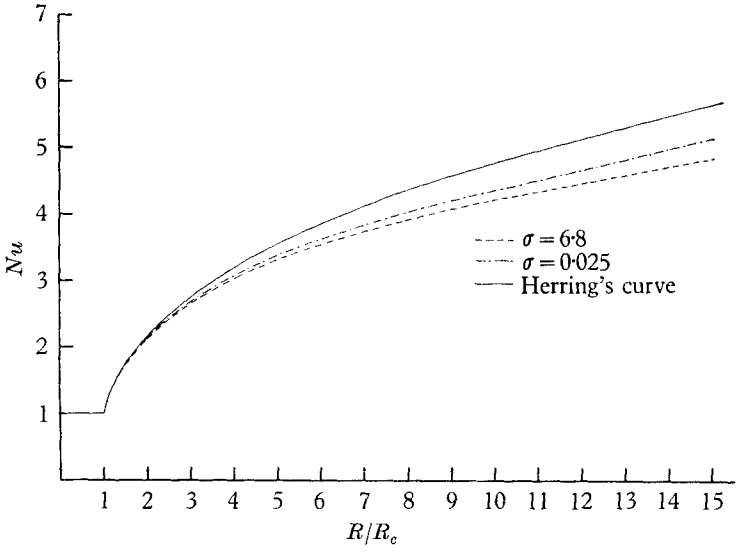

FIGURE 6. Values of Nu *vs.* R/R_c up to $R = 15R_c$ for the cases $\sigma = 6{\cdot}8$ and $\sigma = 0{\cdot}025$ are compared with Herring's values (upper curve).

these non-linear terms leads to a heat transport which is significantly higher than that derived from the complete system. The percentage variation is larger at larger Rayleigh numbers. At $R = 15R_c$ Herring's result for the convective heat flux is 20 % larger than the value for $\sigma = 6{\cdot}8$ and the discrepancy can be expected to increase for larger R. Herring's calculations give numerical solutions of the model equations proposed by Malkus (1954) and were not intended to give exact results. However, his equations are much simpler than the complete system and they provide a remarkably good first approximation to the heat flux.

One conclusion from the foregoing comparison is that the non-linear terms which do not involve, or contribute to, the mean temperature field decrease the heat flux. This was Malkus's (1954) hypothesis about the role of these non-linear terms in his theory of turbulent convection.

In Herring's calculations the mean temperature field had a region of positive gradient just outside the sharp gradient region near the boundaries. From the present results we note that this positive gradient is not removed by the action of the fluctuating non-linear terms.

7. Discussion of the results

We discuss here the implications of some of the qualitative results of the foregoing investigation.

Since all of the integrations settled to a steady state, it appears likely that further calculations for much higher Rayleigh numbers would show steady-state behaviour. Deardorff's (1964) study of the two-dimensional system at a Rayleigh number of 675,000 also showed steady-state behaviour. Apparently the two-dimensionality of the system must be relaxed to allow for vortex stretching in order for transient motions to be maintained. However, admitting possible phase shifts through a treatment of multiple, overlapping, two-dimensional rolls may give rise to transient behaviour. We can only speculate about this possibility at present since it is evident that calculations must be performed to settle the issue.

It has been speculated in the past (Ledoux, Schwarzschild & Spiegel 1961; Kraichnan 1962; Spiegel 1965) that when the Prandtl number is small, as it is for stars ($\approx 10^{-9}$), heat is transported largely by molecular or radiative processes. From our results we find that the convective heat flux is largely independent of σ but the direction of change shows an increase of heat flux with decreasing σ. Furthermore, the mean temperature profile is as distorted by convective processes for small σ as for large. Thus, our results show a qualitative dependence which does not agree with the more heuristic arguments used by workers in the past.

It is possible to give a plausible argument to show why the present results differ from those deduced from the assumption that the fluid is turbulent. In the latter case we assume that heat is transported upward by blobs of fluid. It is plausible in this case to assume that the kinetic energy which is generated is due solely to the conversion of the potential energy of the stratification. The vertical velocity then corresponds to the free-fall velocity. Between the bottom boundary and the top of the bottom boundary layer the temperature changes by an amount at most equal to $\frac{1}{2}\Delta T$. Thus the potential energy of a warm blob of fluid near the bottom boundary can be evaluated as $PE \leqslant \frac{1}{2}g\rho\alpha\Delta T d$. If we assume that this potential energy is converted completely to vertical kinetic energy, we have

$$w^2 \leqslant g\alpha\Delta T d. \tag{7.1}$$

Hence

$$w \leqslant \sqrt{(g\alpha\Delta T d)}. \tag{7.2}$$

The vertical heat flux can be derived from the heat equation

$$H = \kappa\Delta T/d + \langle\overline{wT}\rangle, \tag{7.3}$$

where the superbar corresponds to a vertical average. Now, writing

$$T \sim \tfrac{1}{2}\Delta T \tag{7.4}$$

and assuming that w and T are in phase, we have

$$H \leqslant d^{-1}\kappa\Delta T[1 + \tfrac{1}{2}\kappa^{-1}(g\alpha\Delta T d^3)^{\frac{1}{2}}], \tag{7.5}$$

or

$$H \leqslant d^{-1}\kappa\Delta T(1 + \tfrac{1}{2}(R\sigma)^{\frac{1}{2}}). \tag{7.6}$$

Hence, the maximum convective heat flux at a given value of R is proportional to $\sqrt{\sigma}$ and will consequently decrease as σ decreases. In the limit of small σ we would then have

$$H \approx \kappa\Delta T/d; \tag{7.7}$$

that is, heat is transported by conduction alone. It is also evident that the temperature profile is linear in this case because the distorting term $\langle wT \rangle$ tends to zero as σ does. As a consequence, the estimates (7.2) and (7.4) for w and T are obviously too large so that we have only a weak upper bound on the expression for the heat transport. But the point is that it *is* an upper bound and nevertheless decreases as σ decreases. Incidentally, it is interesting to note that expression (7.6) gives the same dependence on Rayleigh number for the convective heat flux as Howard (1963) derives as a first approximation. Thus our crude estimate is in agreement with the conclusions of other workers but it is at odds with our numerical results.

Now fixing the Rayleigh number and varying σ can be achieved by allowing κ to change but keeping $\Delta T/\kappa$ as well as g, α, ν and d constant. Hence (7.2) can be rewritten as

$$w \leqslant \sqrt{(g\alpha \Delta T d)} \equiv (R\nu d^{-2}\kappa)^{\frac{1}{2}}. \tag{7.8}$$

Thus for the heuristic model w behaves like $\sqrt{\kappa}$.

In our numerical calculations we note that the velocity, w, was non-dimensionalized by $w = \kappa d^{-1} w'$. The amplitudes of w' for the case $R = 20R_c$ were 31·1 for $\sigma = 6{\cdot}8$ and 32·3 for $\sigma = 0{\cdot}005$; i.e. a change of 3 orders of magnitude in σ produced a negligible change in w'. Thus we may conclude that w' is effectively constant and therefore w behaves like κ. Hence, the magnitude of w corresponds to the square of the free-fall velocity.

The foregoing argument accounts for the discrepancy between our numerical results and those deduced for fully turbulent flow. The different behaviours are associated with the form of the motion and temperature fields. In the case of the single cell fluid particles receive positive buoyancy from the lower boundary, move upward and are driven horizontally to the region of descent as they give up their excess heat and acquire negative buoyancy. In this sense they are 'memory' particles and can be accelerated through repeated cycles of motion. Turbulent blobs receive an injection of positive (negative) buoyancy near the lower (upper) boundary, attain a free-fall velocity and then are destroyed. For each cycle the process must begin anew and particles have no memory of their history. Hence, inertial processes can cause the particles to accelerate to a velocity faster than the free-fall velocity in the case of single large cells but not when the flow is turbulent.

Finally we recall that the structure of the mean temperature field shows a reversal of gradient in the body of the fluid. The convective inertia of the temperature field is fundamental in giving rise to this reversal. Certainly one would expect *a priori* to see a monotonic gradient but the present calculation shows this not to be the case for two-dimensional motions. The plausibility argument given earlier for the behaviour of H on small σ in fully turbulent flow showed that the mean temperature profile is essentially linear in this limit. A more quantitative analysis for arbitrary σ would appear to be necessary to show whether there is a region of stable stratification. If the structure of the mean temperature field as deduced here carries over to the three-dimensional turbulent case, it is possible that oscillatory motions can be generated because at least in part of the fluid a restoring force is available to maintain gravitationally stable oscillations. This point may be important in trying to construct theories of large-scale horizontal motions in geophysical phenomena where the sign

of the vertical temperature gradient plays a fundamental role in determining the motions which may be possible.

I am indebted to Dr R. Jastrow, who generously made available the computing facilities at the NASA Institute for Space Studies; Mrs J. Webster for programming some of the subroutines; Mr P. Schneck for his continuous assistance with the program and for applying his profound knowledge of the 7094 system to make the program more efficient; Mr P. Calderone for his help in scheduling the runs and getting the results out quickly; Professor M. Stern for a discussion leading to the turbulent model in § 7; and the National Science Foundation for support under contract no. GP 2564.

REFERENCES

DEARDORFF, J. W. 1964 A numerical study of two-dimensional parallel-plate convection. *J. Atmos. Sci.* **21**, 419.

HERRING, J. 1963 Investigation of problems of thermal convection. *J. Atmos. Sci.* **20**, 325.

HOWARD, L. N. 1963 Heat transport by turbulent convection. *J. Fluid Mech.* **17**, 405.

JAKOB, M. 1949 *Heat Transfer*, vol. 1. New York: Wiley.

KRAICHNAN, R. H. 1962 Turbulent thermal convection at arbitrary Prandtl number. *Phys. Fluids*, **5**, 1374.

KUO, H. L. 1961 Solution of the non-linear equations of motion of cellular convection and heat transport. *J. Fluid Mech.* **10**, 611.

LEDOUX, P., SCHWARZSCHILD, M. & SPIEGEL, E. A. 1961 The spectrum of thermal turbulence. *App. Math. J.* **133**, 184.

MALKUS, W. V. R. 1954 The heat transport and spectrum of thermal turbulence. *Proc. Roy. Soc.* A, **225**, 196.

MALKUS, W. V. R. & VERONIS, G. 1958 Finite amplitude cellular convection. *J. Fluid Mech.* **4**, 225.

SCHLÜTER, A., LORTZ, D. & BÜSSE, F. 1965 On the stability of steady finite amplitude convection. *J. Fluid Mech.* **23**, 129.

SPIEGEL, E. A. 1965 The theory of turbulent convection, presented at the 5th Cosmical Gas Dynamics Symposium in Nice.

VERONIS, G. 1965*a* On finite amplitude instability in thermohaline convection. *J. Mar. Res.* **23**, 1.

VERONIS, G. 1965*b* A note on the use of a digital computer for doing tedious algebra and programming. *Comm. of the ACM*, **8**, 265.

VERONIS, G. 1966 Motions at subcritical values of the Rayleigh number in a rotating fluid. *J. Fluid Mech.* **24**, 545.